Genetic and epigenetic determinants establish a continuum of Hsf1 occupancy and activity across the yeast genome

David Pincus[a,†,*], Jayamani Anandhakumar[b,†], Prathapan Thiru[a], Michael J. Guertin[c], Alexander M. Erkine[b,‡], and David S. Gross[b,*]

[a]Whitehead Institute for Biomedical Research, Cambridge, MA 02142; [b]Department of Biochemistry and Molecular Biology, Louisiana State University Health Sciences Center, Shreveport, LA 71130; [c]Department of Biochemistry and Molecular Genetics, University of Virginia, Charlottesville, VA 22908

ABSTRACT **Heat shock factor 1 is the master transcriptional regulator of molecular chaperones and binds to the same *cis*-acting heat shock element (HSE) across the eukaryotic lineage. In budding yeast, Hsf1 drives the transcription of ~20 genes essential to maintain proteostasis under basal conditions, yet its specific targets and extent of inducible binding during heat shock remain unclear. Here we combine Hsf1 chromatin immunoprecipitation sequencing (seq), nascent RNA-seq, and Hsf1 nuclear depletion to quantify Hsf1 binding and transcription across the yeast genome. We find that Hsf1 binds 74 loci during acute heat shock, and these are linked to 46 genes with strong Hsf1-dependent expression. Notably, Hsf1's induced DNA binding leads to a disproportionate (~7.5-fold) increase in nascent transcription. Promoters with high basal Hsf1 occupancy have nucleosome-depleted regions due to the presence of "pioneer factors." These accessible sites are likely critical for Hsf1 occupancy as the activator is incapable of binding HSEs within a stably positioned, reconstituted nucleosome. In response to heat shock, however, Hsf1 accesses nucleosomal sites and promotes chromatin disassembly in concert with the Remodels Structure of Chromatin (RSC) complex. Our data suggest that the interplay between nucleosome positioning, HSE strength, and active Hsf1 levels allows cells to precisely tune expression of the proteostasis network.**

Monitoring Editor
William P. Tansey
Vanderbilt University

Received: Jun 12, 2018
Revised: Oct 1, 2018
Accepted: Oct 11, 2018

This article was published online ahead of print in MBoC in Press (http://www.molbiolcell.org/cgi/doi/10.1091/mbc.E18-06-0353) on October 17, 2018.

†These authors contributed equally to this work.

‡Present address: Department of Pharmaceutical Sciences, College of Pharmacy and Health Sciences, Butler University, Indianapolis, IN 46208.

Author contributions: D.S.G., D.P., and J.A. designed the project. J.A., D.P., and A.M.E. conducted the experiments. D.P., P.T., and M.G. performed the bioinformatics analysis. D.P., J.A., A.M.E., and D.S.G analyzed the data. D.P., J.A., and A.M.E. made the figures. D.S.G. and D.P. wrote the paper.

*Address correspondence to: David Pincus (pincus@wi.mit.edu) and David S. Gross (dgross@lsuhsc.edu).

Abbreviations used: Ac, acetylation; EMSA, electrophoretic mobility shift assay; GEO, Gene Expression Omnibus; GO, gene ontology; HS, heat shock; HSE, heat shock element; Hsf1, heat shock factor 1; NHS, non–heat shock; me, methylation; MEME, Multiple EM for Motif Elicitation; NFR, nucleosome-free region; rapa, rapamycin; RPM, reads per million mapped reads; RSC, Remodels Structure of Chromatin; RT, room temperature; SPMR, signal per million mapped reads; TE, Tris–EDTA; TSS, transcription start site; UAS, upstream activation sequence.

INTRODUCTION

The cellular response to thermal stress is directed by a transcriptional program whose basic components—sequence-specific activator, *cis*-response DNA element, and core target genes—have been conserved since the last common ancestor in the eukaryotic lineage (Verghese *et al*., 2012). Heat shock factor 1 (Hsf1), master activator of the heat shock response, is a winged helix-turn-helix transcription factor that recognizes DNA sequence motifs (heat shock elements) located upstream of genes encoding chaperones and other cytoprotective heat shock proteins (HSPs) (Wu, 1995; Gomez-Pastor *et al*., 2018). HSPs maintain cellular protein homeostasis (proteostasis) and are required in higher concentrations under stressful conditions to contend with unfolded cytosolic and nucleoplasmic proteins. This is principally achieved via Hsf1-mediated transcriptional up-regulation of the genes encoding these proteins. In addition to its evolutionarily conserved role, mammalian HSF1 contributes to oncogenesis by driving distinct transcriptional programs in both tumor cells and their supporting stroma (Dai *et al*., 2007; Mendillo *et al*., 2012; Scherz-Shouval *et al*., 2014). HSF1 function also has been linked to normal development, neurodegenerative disease, and aging

(Neef *et al.*, 2011; Li *et al.*, 2017). Thus, gaining a deeper understanding of Hsf1 biology may inform development of novel approaches to modulate human HSF1.

Hsf1 is subject to multiple layers of regulation, with two shared across multiple phyla. Under nonstressful conditions, Hsf1 exists primarily as a non-DNA-binding monomer in either nucleus or cytoplasm. In response to thermal or other proteotoxic stress, the protein trimerizes and acquires the capacity for high-affinity DNA binding. In higher eukaryotes, the Hsp90 and Hsp70 chaperones (and their cochaperones) as well as the TRiC/CCT cochaperone complex have been suggested as direct repressors of Hsf1 under basal conditions (Abravaya *et al.*, 1992; Zou *et al.*, 1998; Neef *et al.*, 2014). According to this model, the chaperones are titrated away on heat shock by unfolded or misfolded proteins, allowing Hsf1 to trimerize, bind its cognate HSEs, and transactivate *HSP* genes. Although certain details of Hsf1 regulation differ between metazoans and budding yeast (Sorger and Nelson, 1989; Liu *et al.*, 1997), it was recently shown that Hsp70 binds yeast Hsf1 and negatively regulates it. Hsp70 transiently releases Hsf1 in response to thermal stress and then rebinds on exposure to sustained stress, thereby constituting a two-component feedback loop (Zheng *et al.*, 2016; Krakowiak *et al.*, 2018). Hsf1 has also been suggested to be the downstream effector of various signaling cascades. In the case of yeast, phosphorylation positively tunes Hsf1's transactivation of target genes independent of chaperone regulation (Zheng *et al.*, 2016).

Hsf1-regulated, heat shock-responsive genes have served as a paradigm for understanding basic mechanisms of transcription. For example, the existence of paused RNA polymerase II (Pol II) at the 5′-end of genes was first identified at *Drosophila HSP70* (Rougvie and Lis, 1988). Hsf1-regulated genes in *Saccharomyces cerevisiae* use both SAGA and TFIID pathways for activation, although SAGA plays a dominant role (Ghosh and Pugh, 2011; de Jonge *et al.*, 2017; Vinayachandran *et al.*, 2018). In addition, Mediator has been shown to be a key coactivator of Hsf1-driven transcription in both metazoans and yeast (Park *et al.*, 2001; Fan *et al.*, 2006; Singh *et al.*, 2006; Kim and Gross, 2013). Dynamic genewide eviction of nucleosomes and their subsequent redeposition has been observed at *HSP* genes in both yeast and *Drosophila* (Zhao *et al.*, 2005; Petesch and Lis, 2008; Kremer and Gross, 2009). Recently, Hsf1-regulated yeast genes were observed to undergo striking alteration in their local structure and engage in highly specific *cis*- and *trans*-intergenic interactions on their transcriptional activation, coalescing into discrete intranuclear foci (Chowdhary *et al.*, 2017, 2018).

In budding yeast, the Msn2 and Msn4 gene-specific transcription factors drive transcription of a large set of genes (200–300) in response to a variety of environmental stresses, including heat, oxidative, osmotic, and salt stress (Gasch *et al.*, 2000; Elfving *et al.*, 2014). Msn2/Msn4-regulated genes include several *HSP* genes, but the Msn2/Msn4 regulon is by and large distinct from that controlled by Hsf1. Nonetheless, the identity of the genes whose acutely induced expression is under the direct control of Hsf1 remains unclear. Prior global localization studies of Hsf1 have either lacked resolution or did not evaluate Hsf1 occupancy beyond the basal or chronically induced states (Lee *et al.*, 2002; Hahn *et al.*, 2004; Solis *et al.*, 2016; de Jonge *et al.*, 2017).

Here we investigate the link between Hsf1 occupancy, its function, and the epigenetic determinants underpinning its genome localization under basal, acute, and chronic heat shock states. Our results reveal that Hsf1 binds to a core set of 43 loci under control conditions and that the vast majority of these and 31 others are occupied at substantially higher levels following heat shock; of these 74 bound loci, 46 are associated with genes whose transcriptional activation is Hsf1 dependent. Additionally, our analysis reveals a central role played by preset nucleosome positioning and Remodels Structure of Chromatin (RSC) complex in regulating yeast's dynamic transcriptional response to heat shock.

RESULTS

Yeast Hsf1 binds inducibly to the vast majority of its target genomic sites

To investigate Hsf1 DNA binding genomewide, we performed chromatin immunoprecipitation sequencing (ChIP-seq) to determine where and how strongly it binds under basal (non–heat shock [NHS]), acute heat shock (HS), and chronic heat shock states. To circumvent problems typically encountered when quantifying ChIP-seq data that combine dynamic protein binding with high coverage over a small genome, we performed parallel IPs using both anti-Hsf1 serum as well as preimmune serum at all time points, and we generated paired-end sequencing data to determine the full sequence of the captured fragments (see *Materials and Methods*). Analytically, we subtracted signal from the matched preimmune samples, used only properly paired reads, and allowed for duplicate reads when quantifying fragment pileups. Such an approach revealed that Hsf1 binding could be detected under NHS conditions (30°C) and was centered ~200 base pairs upstream of the transcription start site (TSS) (Figure 1A). In cells exposed to acute heat shock (30° to 39°C shift for 5 min), Hsf1 occupancy increased at least fourfold genomewide and remained elevated in cells chronically exposed (2 h) to the higher temperature. Replicate locus-specific and genomewide occupancy profiles are provided in Figure 1B and Supplemental Figure S1A, which illustrate both the specificity and reproducibility of our ChIP-seq analysis.

Two sets of Hsf1 genomic targets were identified. A core set, composed of 43 loci, was occupied under all conditions, with occupancy typically increased in cells exposed to thermal stress (Figure 1, C and E). A second set, composed of 31 loci, showed subthreshold occupancy under NHS conditions but was inducibly occupied following acute HS; of these, 24 remained Hsf1 bound in cells chronically exposed to thermal stress (Figure 1, C and G). We performed locus-specific chromatin immunoprecipitation (ChIP) to validate examples of each (Supplemental Figure S1B and unpublished data). The core set of Hsf1 targets was enriched for proteostasis components in the cytosol, endoplasmic reticulum (ER), and mitochondria (Figure 1D). Notably, within these 43 core targets, we observed strong inducible binding with a broad range of inducible levels—up to 50-fold at select sites (Figure 1E). Indeed, all but five core targets exhibited elevated occupancy. Thus, yeast Hsf1 inducibly binds 69/74 of its genomic targets on heat shock.

Analysis of the regions occupied by Hsf1 pulled out a sequence of 20 base pairs composed of tandem inverted repeats of NTTCT as the most enriched motif (Figure 1F). This motif is consistent with previous characterization of HSEs from other organisms (Xiao *et al.*, 1991; Leach *et al.*, 2016; Vihervaara *et al.*, 2017). Among the heat-shock-only Hsf1 binding sites, there was a modest enrichment for oxidative stress-responsive genes (Figure 1H) but no enrichment for an alternative binding motif.

DNA-bound Hsf1 is differentially active during basal and acute heat shock states

As previous genomewide studies (Lee *et al.*, 2002; Hahn *et al.*, 2004; Eastmond and Nelson, 2006; Solis *et al.*, 2016; de Jonge *et al.*, 2017) failed to define the Hsf1-dependent repertoire of target genes during acute heat shock, we were interested in knowing whether genes with strong heat shock-inducible and heat shock-only binding were in fact

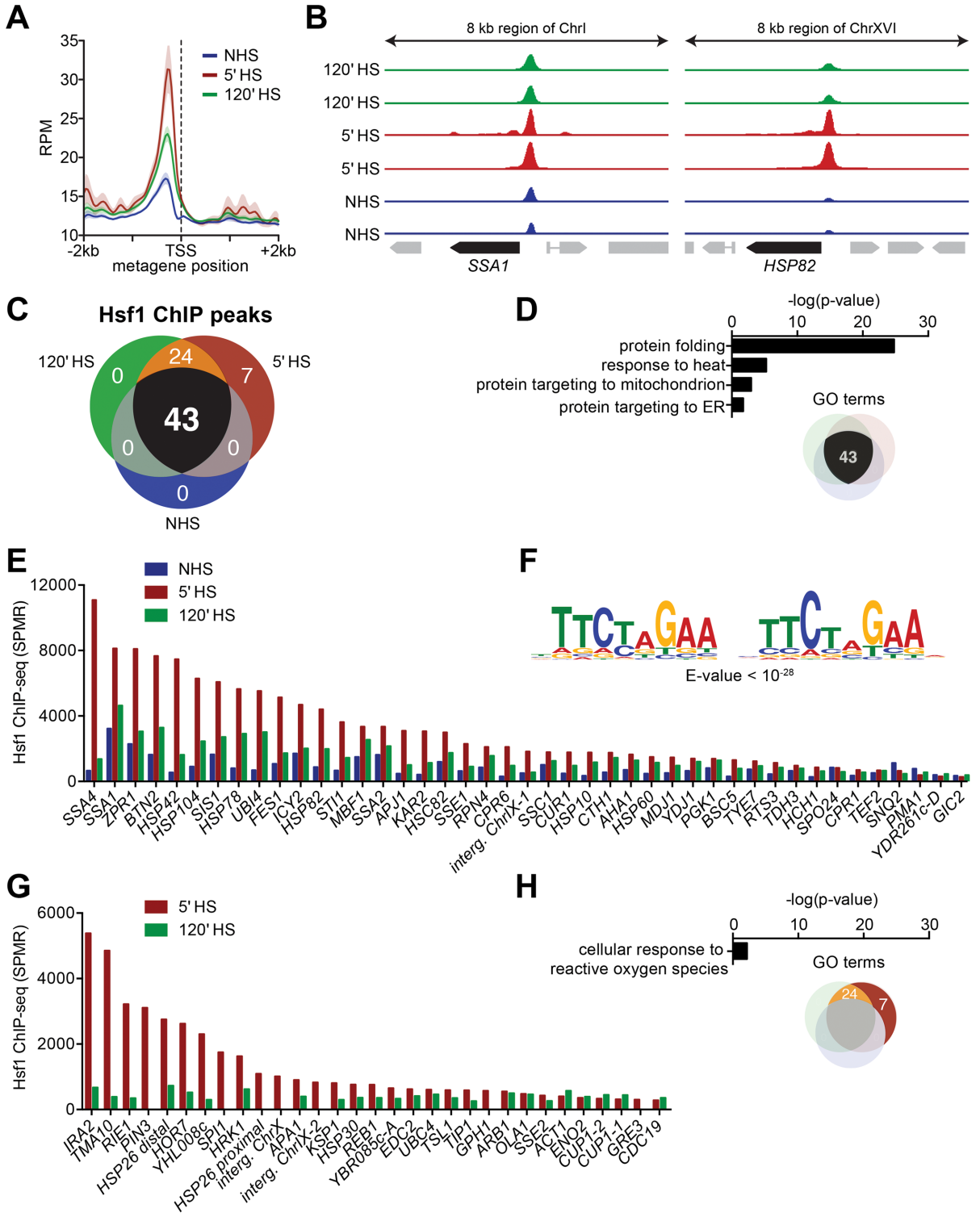

FIGURE 1: Hsf1 ChIP-seq reveals differential basal and heat-shock-inducible binding across the Hsf1 regulon. (A) Metagene plot of Hsf1 ChIP-seq signal genomewide with respect to the TSS under NHS conditions and following 5-min and 120-min HS. Strain BY4741 was used for this and all other Hsf1 ChIP-seq assays in this work. RPM, reads per million mapped reads. (B) IGV browser images of the *SSA1* and *HSP82* loci showing Hsf1 ChIP-seq signal in two biological replicates under NHS conditions and following 5-min and 120-min HS. The *y*-axes are normalized to the maximum displayed signal in the 5-min time point. Preimmune serum ChIP samples (not shown) were used for peak calling (see *Materials and Methods*). (C) Venn diagram showing the number of Hsf1 ChIP peaks that surpassed the background cutoff in both biological replicates under each condition. (D) Gene ontology (GO) term enrichment values for genes immediately downstream of the 43 ChIP peaks. (E) Normalized Hsf1 ChIP signal at the 43 peaks identified under all three conditions; represent the mean of two biological replicates. SPMR, signal per million mapped reads. (F) Consensus motif identified under Hsf1 ChIP peaks detected under all conditions. (G) Normalized Hsf1 ChIP signal at the 31 peaks detected only under HS conditions; presented as in E. (H) GO term enrichment values for the 31 Hsf1 ChIP peaks detected only under HS conditions.

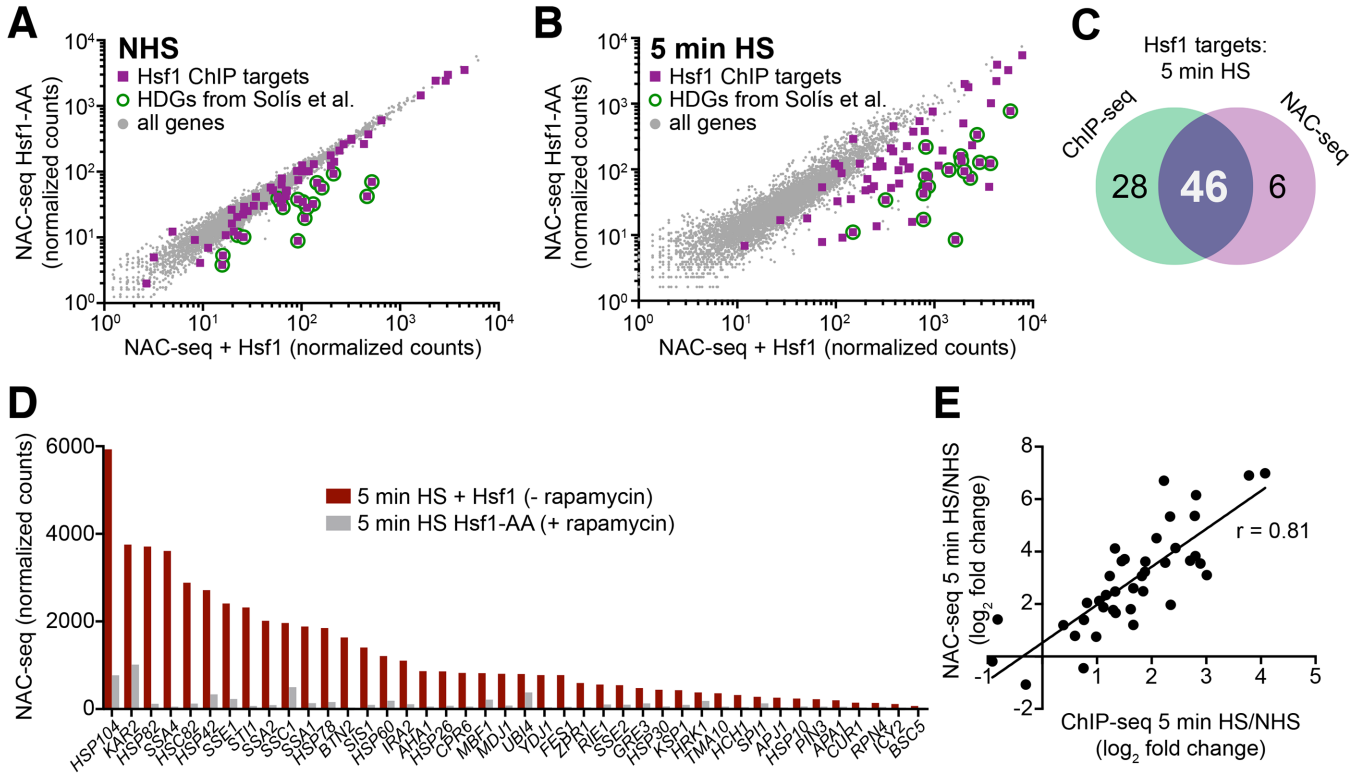

FIGURE 2: NAC-seq coupled with Hsf1-Anchor Away reveals genes dependent on Hsf1 for their basal and induced transcription. (A) NAC-seq counts transcriptome-wide under NHS conditions in the presence and absence of nuclear Hsf1 using the Hsf1 Anchor Away system (Hsf1-AA). Rapamycin (1 μM) was added for 45 min to deplete Hsf1 from the nucleus. Purple squares are genes with Hsf1 ChIP peaks; green circles show Hsf1 targets identified previously under NHS conditions (Solis *et al.*, 2016). Genes with Hsf1 ChIP peaks above background (≥250 SPMR) and whose expression was significantly reduced by rapamycin treatment ($p < 0.01$; two-tailed *t* test) were designated as Hsf1-dependent genes (HDGs). Eighteen fell into this category: *AHA1*, *BTN2*, *CUR1*, *CPR6*, *FES1*, *HCH1*, *HSC82*, *HSP104*, *HSP42*, *HSP78*, *HSP82*, *MBF1*, *MDJ1*, *SIS1*, *SSA1*, *SSA2*, *STI1*, and *YDJ1*. (B) Analysis, representation, and designations as in A, except following 5 min HS. (C) Venn diagram comparing Hsf1 ChIP-seq gene targets and NAC-seq targets following a 5-min HS. ChIP-seq gene targets were derived from 74 total peaks, three of which were intergenic, two of which were linked to a single gene (*HSP26*), and four of which were linked to Hsf1-dependent, bidirectionally transcribed genes (see Figure 3, B and C). (D) NAC-seq counts for shared ChIP-seq/NAC-seq Hsf1 targets following a 5-min HS in the presence and absence of nuclear Hsf1. (Note: NAC-seq counts represent total nascent transcription and are not normalized for gene length.) Only one gene from the four Hsf1-dependent bidirectional genes is shown. (E) Scatter plot showing the correlation between HS-inducible Hsf1 DNA binding and HS-inducible transcription of shared ChIP-seq/NAC-seq Hsf1 targets. ChIP-seq signals represent the mean of two biological replicates.

dependent on Hsf1 for their transcriptional induction. To test this, we deployed a yeast strain in which we could rapidly induce nuclear export of Hsf1 using the Anchor-Away system (Haruki *et al.*, 2008; Solis *et al.*, 2016). Analysis of genomewide transcription rates under NHS and 5 min HS states using nascent mRNA sequencing (NAC-seq; see *Materials and Methods*) revealed that the basal transcription of 18 genes was Hsf1 dependent (Figure 2A), consistent with previous observations (Solis *et al.*, 2016), while heat shock-induced transcription of this set of genes plus an additional 34 were also Hsf1 dependent (Figure 2, B–D; Supplemental Table S1). Most of these genes (46/52) were also occupied by Hsf1 in 5 min heat-shocked cells (Figure 2C), arguing that this set of genes, derived from both core and inducible categories (Figure 1, E and G), is directly regulated by Hsf1. The remaining six genes exhibited subthreshold Hsf1 occupancy. While not meeting our stringent cut-off (see *Materials and Methods*), these six, which include the Hsp70-encoding *SSA3* gene, may be direct targets of Hsf1 as well (see Supplemental Figure S1B). The 28 Hsf1 targets whose transcription was Hsf1 independent are largely composed of highly expressed housekeeping genes (Supplemental Figure S2) that are presumably controlled by multiple gene-specific, functionally redundant activators. Notably, for the 46 genes corroborated by both ChIP-seq and NAC-seq, induced DNA binding by Hsf1 led to a disproportionate increase in nascent transcription during the first 5 min of heat shock (typically 7.5-fold and in certain cases nearly 20-fold [Figure 2E]) (see *Discussion*).

Examination of individual Hsf1-dependent genes revealed surprising variation with respect to their genomic arrangement and transcriptional response. Some, such as *HSC82* and *SSA2*, were exclusively activated by Hsf1 and, as revealed by Anchor Away, entirely dependent on it for their expression (Figure 3A; compare NAC-seq tracks –/+ Hsf1 [see also Figure 2D]). Others, such as genes within the bidirectional pairs *SIS1-LST8* and *YGR210C-ZPR1*, were symmetrically activated and Hsf1 dependent (Figure 3B). However, the gene pairs *HSP82-YAR1* and *SSC1-TAH11* were asymmetrically activated, with one gene strongly induced while the other only weakly, yet both members were Hsf1 dependent (Figure 3C). In the case of *YAR1*, the Pol II transcript began well upstream of the gene, suggesting that this heat-shock-inducible RNA might be noncoding. Since in each case the gene more strongly activated by Hsf1 was positioned closer to the Hsf1 site, the most parsimonious explanation is that proximity of

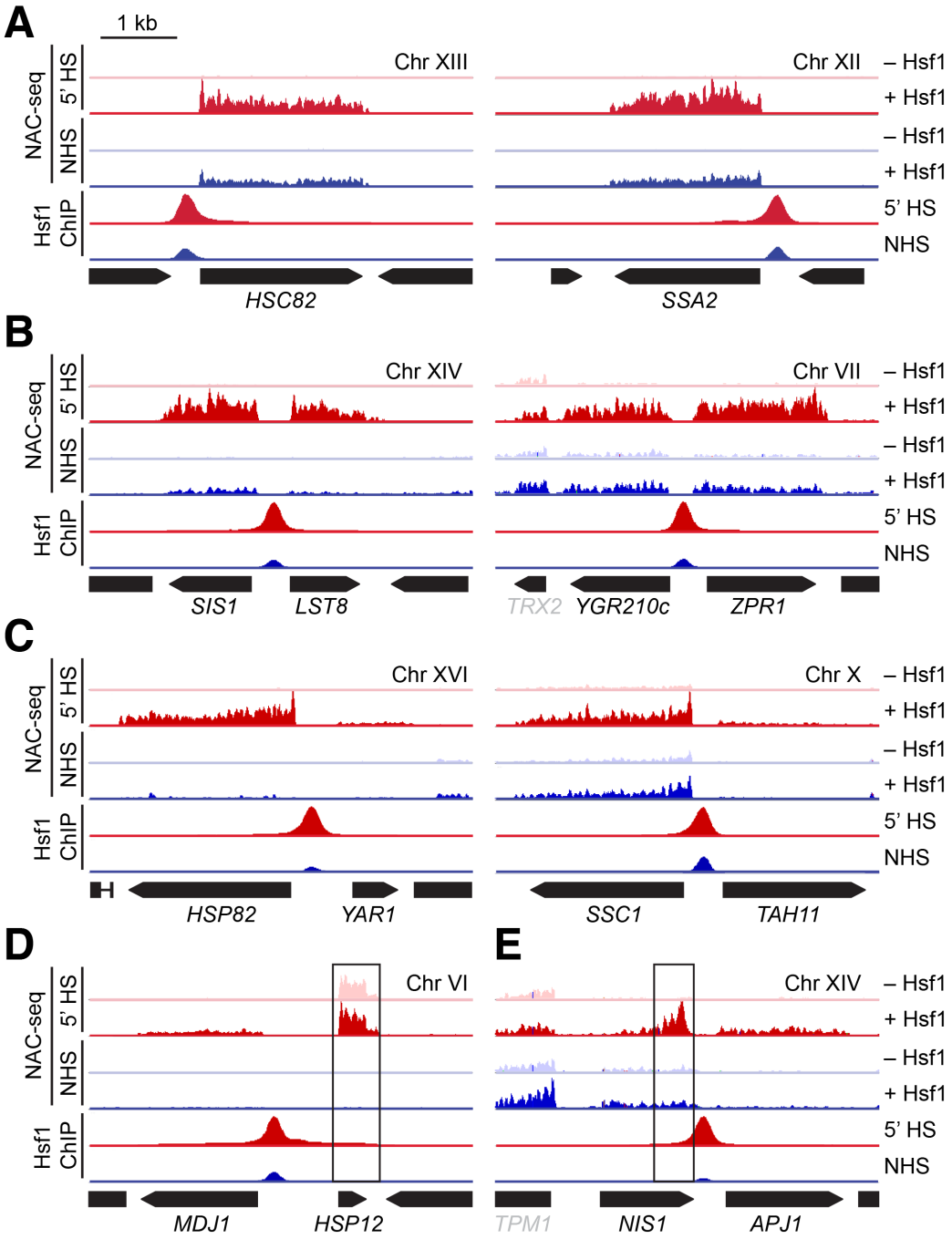

FIGURE 3: Hsf1 stimulates both unidirectional and bidirectional transcription. (A) IGV browser images of 5-kb windows at Hsf1-dependent loci. Tracks show NAC-seq and Hsf1 ChIP-seq under NHS and 5-min HS conditions; NAC-seq was conducted in the presence and absence of nuclear Hsf1 using the Hsf1-AA system. ChIP-seq and NAC-seq tracks were normalized to the maximum displayed value for each locus in the 5-min heat-shock sample. NAC-seq tracks represent both sense and anti-sense transcription yet for simplicity are shown above the line for each gene. Hsf1 was anchored away with 1 μM rapamycin for 45 min. (B) As in A but for loci that show near-stoichiometric, Hsf1-dependent bidirectional transcription. (C) As in B but for loci that show substoichiometric, Hsf1-dependent transcription of the nonchaperone gene. (D) As in C but for the *MDJ1/HSP12* locus on chromosome VI. Although both *MDJ1* and *HSP12* are induced by heat shock, only *MDJ1* is Hsf1 dependent. (E) As in C but for the *NIS1/APJ1* locus on chromosome XIV. Demonstrates heat-shock- and Hsf1-dependent bidirectional transcription in the sense direction for *APJ1* and in the antisense direction for *NIS1*.

the HSE to the core promoter/TSS dictates robustness of Hsf1 activation. The bidirectionally transcribed *MDJ1–HSP12* gene pair is striking for the strong Hsf1 dependence of one gene, *MDJ1*, but not of the other, *HSP12* (Figure 3D; Supplemental Table S1). Indeed, *HSP12* appears to be primarily regulated by the alternative thermal stress-responsive activators Msn2 and Msn4 (Gasch *et al.*, 2000). Also notable is the tandemly oriented *NIS1–APJ1* gene pair. While both genes are heat shock induced and Hsf1 dependent, *NIS1* is

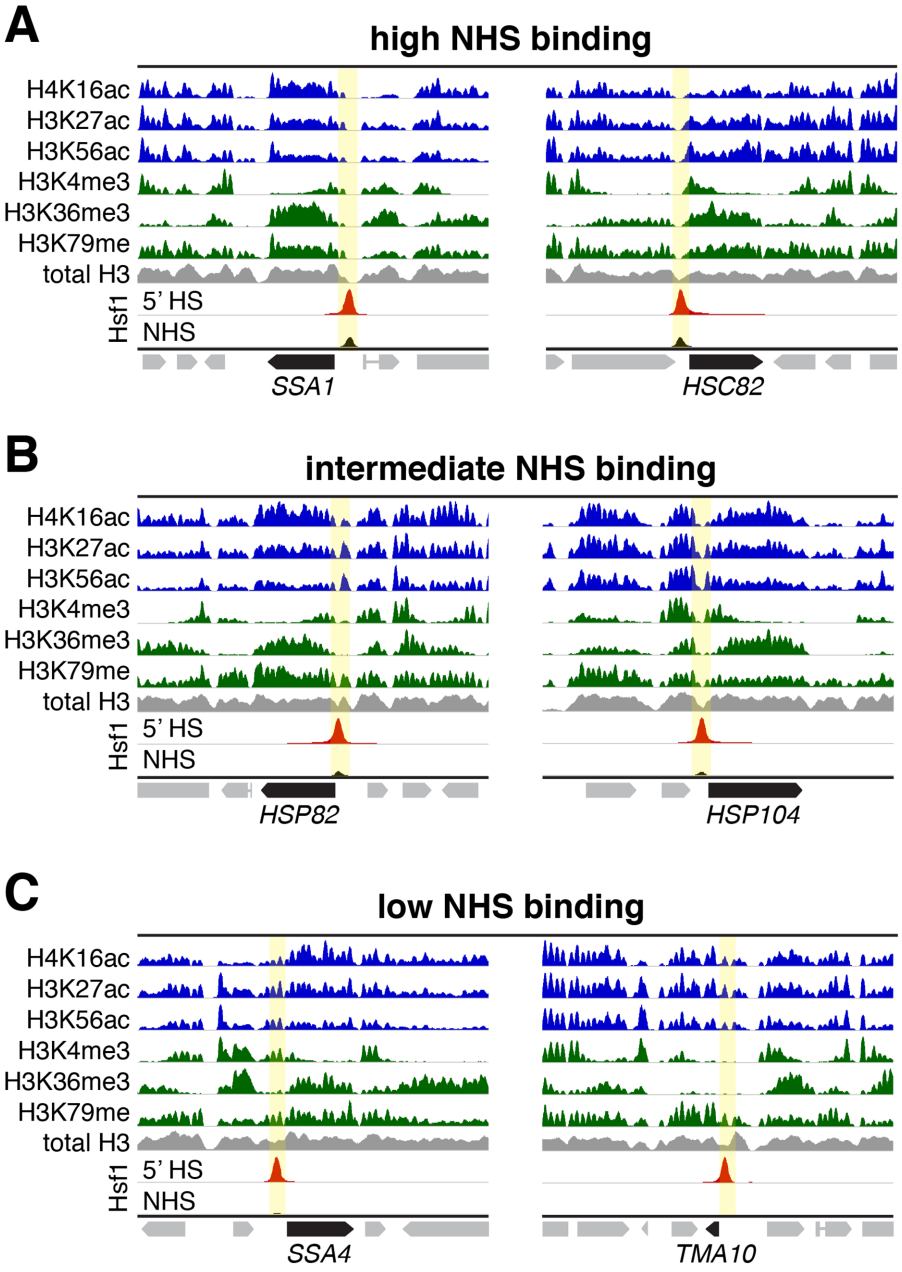

FIGURE 4: Hsf1's constitutive occupancy correlates with preset accessible chromatin, while its heat-inducible occupancy correlates with preexisting histone acetylation and partial nucleosome occupancy. (A) ChIP-seq profiles of the indicated covalently modified histones, total H3 and Hsf1 over 10 kb windows of representative High NHS Binding loci (high Hsf1 occupancy under control conditions). Location of Hsf1 binding peak is highlighted in yellow. All tracks except Hsf1 were normalized to their own maximum displayed signal and are from publicly available data sets (NHS state; see *Materials and Methods*). Hsf1 tracks depict both NHS and 5-min HS states and are normalized to the 5-min HS sample (this study). (B) As in A, except depicted are Intermediate Hsf1 Binding loci. (C) As in A, except depicted are Low Hsf1 Binding loci.

transcribed in the antisense direction (Figure 3E). Thus, Pol II transcripts arising from *YAR1* and *NIS1* are consistent with the idea that Hsf1 directs the expression of heat-shock-inducible lncRNAs.

A preset chromatin state poises Hsf1 for constitutive occupancy of core target loci

As we observed a broad spectrum of Hsf1 binding across the genome under both basal and heat-inducing conditions, we wished to know whether one or more properties of the preset chromatin landscape correlated with this behavior. We examined these at three classes of Hsf1 target genes: 1) those with strong Hsf1 binding under NHS conditions ("High NHS Binding"), 2) those with intermediate Hsf1 binding under NHS conditions ("Intermediate NHS Binding"), and 3) those whose Hsf1 binding was only detectable following 5 min HS ("Low NHS Binding").

High NHS Binding genes such as *SSA1*, *SSA2*, and *HSC82* displayed prominent nucleosome-free regions (NFRs) at the site of Hsf1 binding (Figure 4A and Supplemental Figure S3A; highlighted in yellow). In addition, nucleosomes flanking and/or downstream of these NFRs were enriched in histone marks linked to transcription, including acetylated H2A, H3, H4; H3K4me3; H3K36me3; and H3K79me (Li *et al.*, 2007). While these marks are consistent with the strong basal transcription of these genes (Supplemental Table S1), their enrichment varied between genes. The preset chromatin landscape of Intermediate NHS Binding genes, epitomized by *HSP78*, *HSP82*, and *HSP104* was similar although the breadth of the NFR was noticeably reduced (Figure 4B and Supplemental Figure S3B). This may reflect the smaller proportion of cells with Hsf1 prebound upstream of these genes. Finally, the preset chromatin of Low NHS Binding genes, exemplified by *SSA4*, *HSP26*, and *TMA10*, either lacked an NFR altogether (*SSA4*) or showed a greatly muted NFR (*TMA10*, *HSP26*) (Figures 4C and Supplemental Figure S3C). Instead, the upstream regions of these genes were enriched in histone acetylation marks, while classic methylation marks of transcription (H3K4me3, H3K36me36, and H3K79me3) were depleted. Absence of the latter is consistent with the fact that these genes express at very low levels in NHS cells (Supplemental Table S1). Notably, no class displayed enrichment of the Htz1 (H2A.Z) variant, contrary to models which posit that this histone is enriched at nucleosomes flanking promoter-associated NFRs (Hartley and Madhani, 2009).

The foregoing analysis suggests that a primary determinant of Hsf1 occupancy in NHS cells is whether the upstream region of a target gene is preassembled into stable chromatin. A powerful model to test this idea is the *HSP82* upstream activation sequence (UAS), which is occupied by Hsf1 under basal conditions (Figure 1E and Supplemental Figures S1B and S8A) while also partially assembled into chromatin, as inferred from histone ChIP and ChIP-seq assays (Figures 4B and 5A and Supplemental Figure S8B).

To directly test the ability of yeast Hsf1 to bind nucleosomal DNA, we reconstituted the upstream region of *HSP82* into chromatin using purified HeLa core histones (Supplemental Figure S4; see *Materials*

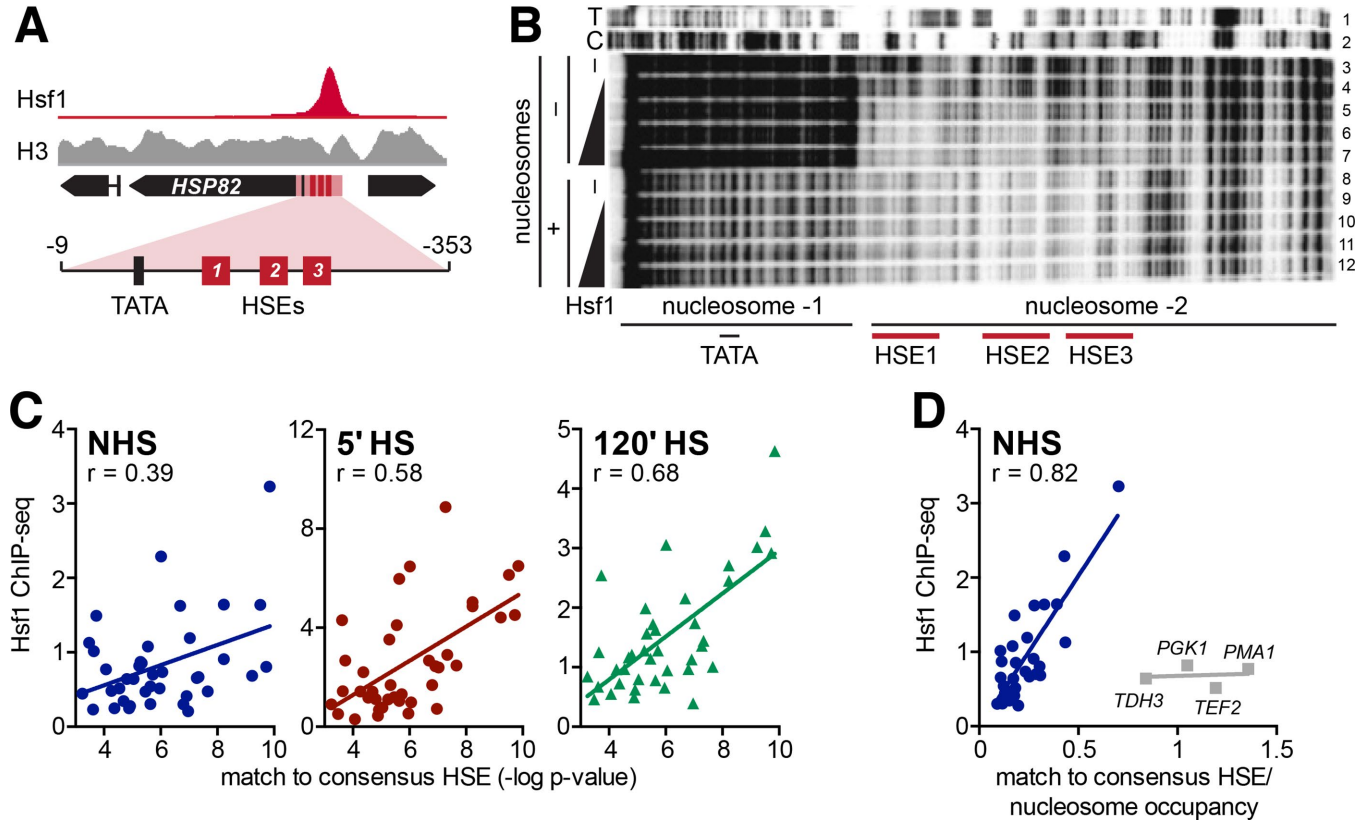

FIGURE 5: Hsf1 DNA binding is impeded by nucleosomes, both in vitro and in vivo. (A) Hsf1 and H3 ChIP-seq signal at *HSP82* under NHS conditions, normalized to their maximum displayed values. The region used for nucleosome reconstitution and DNase I footprinting is highlighted. (B) DNA corresponding to the *HSP82* upstream region depicted in A (spanning –9 to –353 [ATG = +1]) and ^{32}P-end labeled on the upper strand was either reacted directly with GST-Hsf1 (lanes 4–7) or following its reconstitution into a dinucleosome (lanes 9–12). Reconstitution was achieved using a 1:1 (wt/wt) HeLa histone: DNA ratio and salt dilution, followed by purification over a glycerol gradient (see Supplemental Figure S4). Both naked DNA and chromatin templates were challenged with increasing amounts of recombinant Hsf1 (lanes 3 and 8 are -Hsf1 controls) and then subjected to DNase I digestion. DNA was purified and electrophoresed on an 8% sequencing gel. (C) Scatter plots of Hsf1 ChIP-seq signal as a function of the strength of the HSE for the NHS, 5-min HS, and 120-min HS states. HSE strength was determined by MEME as a *p* value corresponding to how well the binding site beneath the summit of each ChIP peak matched the consensus HSE motif (Figure 1F). ChIP-seq signals represent the mean of two biological replicates. (D) As in C, but here each *p* value was divided by the H3 ChIP-seq signal below the summit of the Hsf1 peak under NHS conditions (H3 ChIP-seq data from Qiu *et al.* [2016]). Outliers (gray) consist of Hsf1-independent housekeeping genes.

and Methods). Strikingly, this procedure resulted in the assembly of a dinucleosome composed of one nucleosome centered over the core promoter and a second over the UAS (HSEs1-3) and surrounding region, as revealed by DNase I footprinting (Figure 5B, compare lane 8 with lane 3). The nucleosome over the core promoter appears to be rotationally phased as revealed by the chromatin-specific, ~10-base DNase I cleavage periodicity (Sollner-Webb *et al.*, 1978). Equally striking, this footprinting pattern resembles that obtained by DNase I genomic footprinting of an inactivated allele of *HSP82* (*hsp82-ΔHSE1*) to which Hsf1 cannot bind and whose upstream region is occupied by two strongly positioned nucleosomes (Gross *et al.*, 1993; Venturi *et al.*, 2000). When we challenged this template with recombinant Hsf1, no Hsf1-dependent DNase I footprint could be detected (Figure 5B, lanes 9–12), in contrast to naked DNA, where protection was evident over the entire UAS_{HS} (Figure 5B, lane 3 vs. lanes 5–7). Thus, although recombinant Hsf1 is capable of cooperative, high-affinity binding to the *HSP82* UAS (Figure 5B and Erkine *et al.* [1999]), it cannot bind to the same DNA sequence when it is preassembled into a stable dinucleosome.

Genomewide Hsf1 occupancy is largely dictated by accessible, high-quality HSEs

While the above analysis suggests that preexisting chromatin state plays an important role in dictating Hsf1 occupancy, other parameters, such as the quality of the HSE, may also play a role. To test this, we quantified how well the putative Hsf1-bound sequence under each ChIP peak matched the HSE consensus sequence we derived from all ChIP peaks (TTCTAGAAnnTTCTAGAA; Figure 1F) and compared this score (Supplemental Figure S1C) with the amount of Hsf1 ChIP signal. We found little correlation under NHS conditions, but improved correlation as a function of time during heat shock (120′ > 5′ > NHS) (Figure 5C). Strikingly, when the quality of the HSE was considered in conjunction with nucleosome density as determined by total histone H3 ChIP-seq signal, a strong correlation was found under NHS conditions between this parameter (HSE quality/nucleosome density) and Hsf1 occupancy (Figure 5D, $r = 0.82$). That is, 64% of the variance in Hsf1 ChIP signal across the genome in the control state can be accounted for by HSE quality/nucleosome density alone.

Pioneer transcription factors are enriched within upstream regions of genes with high levels of constitutively bound Hsf1

How are nucleosome-free or nucleosome-depleted regions formed at Hsf1 binding sites? In mammals, "pioneer" transcription factors, epitomized by FoxA1 and related proteins, have been shown to potentiate the subsequent binding of gene-specific activators through their ability to invade repressive chromatin and create locally accessible regions (reviewed in Zaret and Carroll [2011] and Zaret *et al.* [2016]). The DNA binding proteins Rap1, Reb1, and Abf1 (sometimes termed General Regulatory Factors) have similar qualities: abundant, sequence-specific, constitutively bound to DNA and frequently located within nuclease-hypersensitive, open chromatin (Buchman *et al.*, 1988; Chasman *et al.*, 1990; Bai *et al.*, 2011; Ganapathi *et al.*, 2011). We therefore asked whether the genomewide localization of Rap1, Reb1, and Abf1 in the NHS state showed any correspondence to that of Hsf1. As shown in Supplemental Figure S5A, there is a striking enrichment of these factors overlapping or in close proximity to the nucleosome-depleted, high-NHS binding Hsf1 sites of *SSA1* and *HSC82*. This relationship also exists with certain Intermediate NHS Binding Genes (e.g., *HSP82*) although not with others (e.g., *HSP104*) (Supplemental Figure S5B). It is particularly evident at strongly expressed housekeeping genes such as *TEF2* and *TDH3* (Supplemental Figure S5D); at such genes, Hsf1's contribution to transcription is modest, especially under NHS conditions (Supplemental Table S1). In contrast, the Low NHS Binding Genes *SSA4* and *HSP26* were located in Rap1/Reb1/Abf1 deserts with comparatively high H3 occupancy (Supplemental Figure S5C). Overall, there was a modest but significant correlation between the amount of pioneer factor bound within 1 kb upstream of the 43 core Hsf1 targets ($R^2 = 0.26$; $p = 0.0008$) (Supplemental Figure S5E). Together, this analysis suggests that pioneer factor binding is an important factor distinguishing high Hsf1 NHS binding targets from the low NHS binding, heat shock-inducible targets.

Reb1 potentiates open chromatin, Hsf1-transactivation, and Hsf1-mediated nucleosome displacement

To more directly address the role of pioneer factors in fostering Hsf1 binding and activity, we investigated the effect of mutating a high-affinity Reb1 binding site upstream of *HSC82*, creating a mutant allele termed *hsc82-ΔREB1*, and compared it to an isogenic mutant bearing a dual substitution of the two HSEs (termed *hsc82-ΔHSEs*) (Erkine *et al.*, 1996). Hsf1 ChIP-seq and Reb1 ChEC-seq suggest high-level, overlapping occupancy of Reb1 and Hsf1 at *HSC82* under control conditions (Figure 6A) (Zentner *et al.*, 2015). Locus-specific ChIP confirmed this and, moreover, revealed that Reb1 occupancy was modestly diminished by a chromosomal substitution of HSE0 and HSE1 that obviates Hsf1 binding (Figure 6, B and C). Similarly, chromosomal substitution of the Reb1 site, resulting in strongly reduced Reb1 occupancy (Figure 6B), negatively impacted Hsf1 binding (Figure 6C). Interestingly, mutation of the Reb1 site diminished *hsc82* expression greather than sevenfold in nonstressed cells and up to fivefold in acutely stressed ones (Figure 6D), and this corresponded to a pronounced increase (three- to fourfold) in nucleosome occupancy within the UAS and coding region of the gene. Thus, the ability of Hsf1 to remodel chromatin was impaired at *hsc82-ΔREB1*. Likewise, obviating Hsf1 binding led to an increase in H3 occupancy over both UAS and gene coding regions and additionally suppressed the eviction of histones that takes place during heat shock (Figure 6E). Collectively, the data suggest that pioneer factors functionally cooperate with Hsf1 at select genes. In the absence of pioneer factor binding, other factors, including an increase in available Hsf1 (through chaperone titration as described above), are still able to drive nucleosome displacement on acute heat shock (schematically summarized in Figure 7).

RSC facilitates nucleosome depletion and Hsf1 binding within pioneer factor deserts

Finally, we asked whether the abundant, ATP-dependent chromatin remodeling complex (CRC), RSC (Cairns *et al.*, 1996), plays a substantive role in creating a favorable chromatin template for Hsf1 binding and HS-dependent chromatin remodeling (Zhao *et al.*, 2005; Zhang *et al.*, 2014). RSC has been shown to remodel a nucleosome covering Gal4 binding sites, rendering these sites accessible and, as a consequence, the linked *GAL1* and *GAL10* genes responsive to Gal4 activation (Floer *et al.*, 2010). Using Anchor Away as above, we conditionally depleted Sth1, the catalytic subunit of RSC, from the nuclei of Sth1-FRB tagged cells and then subjected the cells to a subsequent acute heat shock (or not) and evaluated the effect on Hsf1 and H3 occupancy at representative High, Intermediate, and Low NHS Binding genes. Sth1 perturbation minimally affected Hsf1 and H3 occupancy at the High NHS Binding gene, *HSC82*, although it did lead to an increase in H3 occupancy at the Intermediate NHS Binding gene, *HSP104* (Figure 6, F and G). Interestingly, at the Low NHS Binding gene, *TMA10*, both Hsf1 and H3 occupancy were significantly affected (Figure 6H). These results suggest that RSC plays an increasingly important, nonredundant role in Hsf1-mediated regulation of genes whose preset chromatin structure is antagonistic to Hsf1 occupancy and function.

DISCUSSION

Yeast Hsf1 inducibly binds DNA genomewide in response to thermal stress

Results presented here indicate that Hsf1 binds heat-inducibly to the vast majority of its transcriptional targets (69/74). While seemingly contrary to original claims that yeast Hsf1 constitutively binds HSEs, based on EMSA (Sorger *et al.*, 1987), genetic analysis (Jakobsen and Pelham, 1988), or genomic footprinting (Gross *et al.*, 1990), in fact our data validate that a small fraction (~25%) of Hsf1 constitutively binds select HSEs even under NHS conditions. This is consistent with the ability of yeast Hsf1 to trimerize under cell-free conditions (Sorger and Nelson, 1989). Isolation of cell lysates or nuclei (prerequisite for EMSA and genomic footprinting) require spheroplasting, a procedure that induces the heat shock response (Adams and Gross, 1991), thereby providing a plausible explanation for the earlier claims. In vivo dimethyl sulfate footprinting analysis provided initial evidence for inducible Hsf1 binding in *S. cerevisiae* (Giardina and Lis, 1995).

Hsf1's occupancy under NHS conditions, while correlating poorly with the quality of the bound HSE, shows a striking correlation to a related parameter, quality of HSE/nucleosome occupancy ($r = 0.82$). Consistent with this, recombinant Hsf1 cannot bind HSEs assembled into a stable nucleosome, even one that has been reconstituted with hyperacetylated histones (A.M.E. and D.S.G., unpublished observations). Thus, other factors must come into play, and we demonstrate that a preset, nucleosome-free (or depleted) chromatin structure typifies the upstream regions of High NHS Binding genes. One attribute underpinning the NFRs of high Hsf1 occupancy promoters is the presence of constitutively bound pioneer factors Rap1, Reb1, and Abf1. These abundant, DNA-binding proteins are overrepresented at such genes, while unrepresented at Low NHS Binding genes. They may work through recruitment of CRCs that mediate the nucleosome-free state (Krietenstein *et al.*, 2016). Alternative sequence-specific factors may serve an analogous

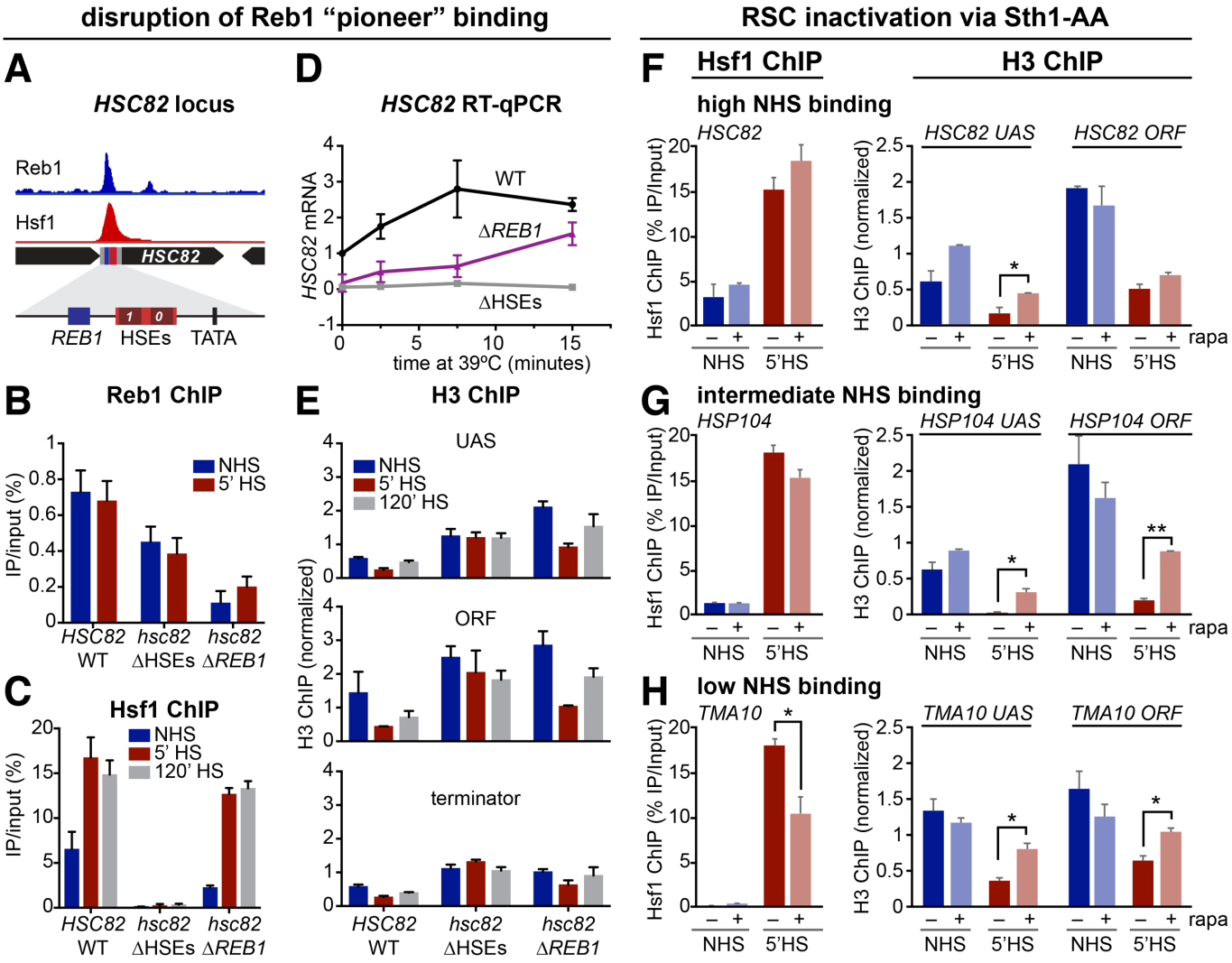

FIGURE 6: The pioneer factor Reb1 enables Hsf1 binding to a high NHS binding target while RSC cooperates with Hsf1 to displace nucleosomes during heat shock. (A) Browser shot showing Reb1 ChEC-seq (Zentner *et al.*, 2015) and Hsf1 ChIP-seq signal under NHS conditions at a 5-kb window around the *HSC82* locus. Both tracks are normalized to their maximum displayed values. Expanded view of the *HSC82* promoter shows the locations of the Reb1 binding site, HSEs, and TATA box (centered at –249, –193, and –138, respectively; ATG = +1). (B) Reb1-myc9 ChIP-qPCR analysis of the *hsc82* promoter under NHS and 5-min HS conditions in isogenic *HSC82*, *hsc82*-ΔHSEs, and *hsc82-ΔREB1* cells conducted as described under *Materials and Methods*. The *hsc82*-ΔHSEs allele bears multiple point substitutions within HSE0 and HSE1 while *hsc82-ΔREB1* bears a 10-base-pair chromosomal substitution of the Reb1 binding site (Erkine *et al.*, 1996). Shown are means + SD ($N = 2$ biological replicates; qPCR = 4). (C) Hsf1 ChIP analysis of the *hsc82* UAS region, conducted and analyzed as in B. (D) Quantification of *HSC82* mRNA expression level by RT-qPCR over a heat-shock time course. Plotted are means ± SD ($N = 2$; qPCR = 4). (E) Histone H3 ChIP analysis of the *HSC82* promoter, midcoding region (open reading frame [ORF]), and 3′-UTR-terminator region. H3 ChIP signals were normalized to those detected at a nontranscribed locus, *ARS504*, which served as an internal recovery control. (F–H) Hsf1 and H3 ChIP at *HSC82*, *HSP104*, and *TMA10* (as indicated) under NHS and 5-min HS conditions, in the presence and absence of the RSC catalytic subunit, Sth1 (rapa – and rapa +, respectively). Conditional nuclear depletion of Sth1 was achieved using an Sth1-AA strain that was pretreated with 1 μM rapamycin (rapa) for 2.5 h. Analysis and display as in B. *, $p < 0.05$; **, $p < 0.01$, two-tailed *t* test.

role at High NHS Binding genes such as *ZPR1* with low occupancy of Rap1, Reb1, and Abf1 (Supplemental Figure S5E).

At Low NHS Binding Genes, relocalization of RSC that occurs on heat shock (Vinayachandran *et al.*, 2018) may be enhanced by the presence of poly(dA-dT) motifs (Lorch *et al.*, 2014) that are significantly enriched within the NFRs of these genes (Supplemental Figure S6). Given that our evidence argues against a dominant role for RSC, Hsf1 likely recruits multiple CRCs (Zhao *et al.*, 2005; Shivaswamy and Iyer, 2008; Krietenstein *et al.*, 2016). In addition, heat shock–activated Hsf1 triggers widespread changes in the genome that may contribute to its ability to occupy nucleosomal genomic sites and expand its regulon. Hsf1-target genes engage in frequent intergenic (both *cis*- and *trans*-) interactions during acute heat shock; such coalescence is strictly dependent on Hsf1 and encompasses High NHS, Intermediate NHS, and Low NHS genes (Chowdhary *et al.*, 2017, 2018). *HSP* gene coalescence may be indicative of liquid–liquid phase separation postulated to underlie transcriptional control in higher eukaryotes (Hnisz *et al.*, 2017). Thus, it could be hypothesized that

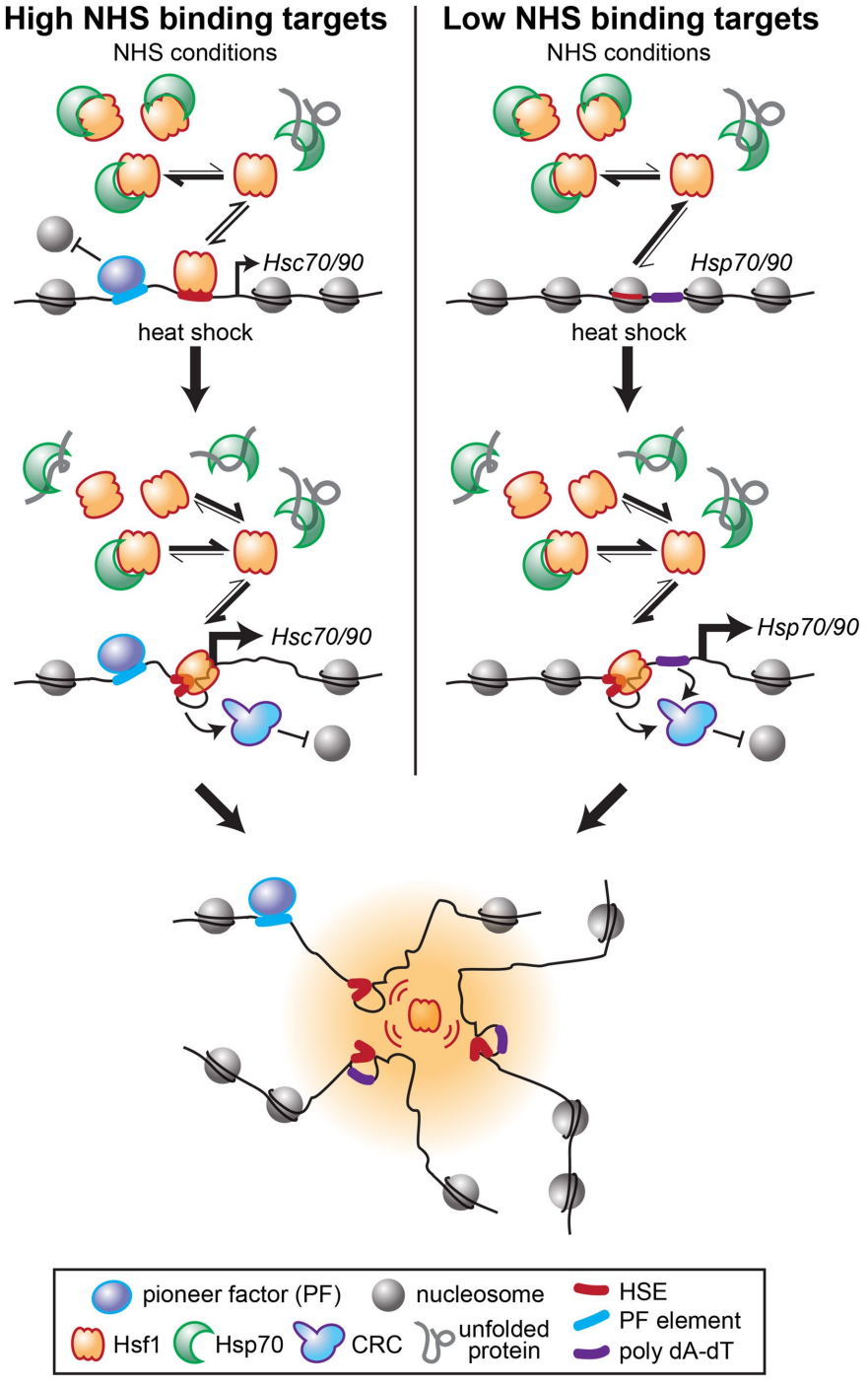

FIGURE 7: Model for differential basal and inducible Hsf1 binding across the genome. Target genes with high levels of Hsf1 binding under non-heat-shock conditions (High NHS binding targets) have nucleosome-free (or depleted) regions upstream of the TSS due to the presence of pioneer factors. Such NFRs are occupied by the small fraction of DNA binding-competent Hsf1 present, stimulating basal transcription of linked *HSC70/90* genes (e.g., *SSA1, SSA2, HSC82*). These genes nonetheless show approximately twofold increases in Hsf1 binding on acute heat shock when the bulk of Hsf1 is liberated from repressive association with Hsp70. This inducible binding further restructures the loci and drives increased transcription. In contrast, Low NHS binding targets (e.g., *SSA4, HSP26, TMA10*) lack proximal pioneer factor binding, and Hsf1 binding sites are occluded by nucleosomes. The fraction of free Hsf1 available under NHS conditions is insufficient to invade the chromatin at these sites. On heat shock, the large increase in DNA-binding competent Hsf1 allows Hsf1 to cooperatively bind its cognate HSEs, and along with poly(dA-dT) tracts that help recruit CRCs, to restructure the loci and drive high-level transcription. Active Hsf1 then drives looping and coalescence of its target loci into transcriptionally active foci that may form phase-separated assemblies.

the high local concentration of Hsf1 liberated from Hsp70 on heat shock would enable Hsf1 to gain a toehold at inducible targets and begin to recruit Mediator and other coactivators (many of which, like Hsf1 itself, harbor intrinsically disordered regions), driving coalescence among targets. These "Hsf1 bodies" could serve as a platform to recruit RSC and other CRCs through protein–protein interactions centered at coalesced UAS/promoters (see model in Figure 7).

DNA-bound Hsf1 exists in multiple, functionally distinct states

An important implication of our study is that DNA-bound Hsf1 significantly differs in its ability to stimulate transcription of its targets depending on the proteotoxic state of the cell. Under control conditions, a core set of 43 genes is detectably occupied by Hsf1. Following acute HS, most of these 43 are occupied at substantially higher levels (genome-wide Hsf1 occupancy increased ≥4-fold). Nascent transcription of these genes increased even more, nearly 30-fold. Thus, DNA-bound Hsf1 exists in a far more active state (~7.5-fold) in acutely stressed cells. A possible basis for this is that the Hsp70 chaperone, shown to bind Hsf1 in whole cell extracts isolated from NHS cells but not from those exposed to 5 min HS (Zheng *et al.*, 2016; Krakowiak *et al.*, 2018), is also associated with DNA-bound Hsf1 under NHS but not acute HS conditions. During more chronic exposures to stress, nascent transcription is reduced (Solis *et al.*, 2016), and this may be accompanied by Hsp70 rebinding to DNA-bound Hsf1 (Zheng *et al.*, 2016).

Related to the above, Hsf1-dependent transcription varies from one promoter to another under a particular condition, even after normalization of ChIP-seq signal (Supplemental Figure S7). What might account for this? Undoubtedly, quality of core promoter elements contributes. However, additional factors might also come into play, such as pioneer factors and/or chromatin remodeling complexes, that may either enhance or suppress the transcription-stimulating activity of DNA-bound Hsf1. One way this could be accomplished is by facilitating the association/disassociation of Hsp70. Especially intriguing is the hyperactive state of Hsf1 bound upstream of the essential basal targets *HSC82* and *SSA2* (Supplemental Figure S7A).

Quality of HSE strongly correlates with Hsf1 binding in heat-shock-induced cells

Earlier work on Hsf1 suggested that its binding avidity and transcriptional activity were linked to the presence of various types of HSEs, termed perfect, gap, step, and direct

repeat (reviewed in Sakurai and Takemori [2007]). However, we have found that only when the role of chromatin is lessened—for example, following nucleosome disassembly that accompanies heat shock (Zhao *et al.*, 2005; Kremer and Gross, 2009)—does a strong correlation exist between Hsf1 occupancy and quality of the HSE (defined as match to the consensus; Figure 5C). Indeed, 7/8 perfect HSEs located within promoter regions were occupied by Hsf1 following acute heat shock, while a far lower fraction of suboptimal HSEs were similarly occupied (e.g., 15/82 TTCnnGAAnnTTC motifs and 13/110 GAAnnTTCnnGAA motifs; Supplemental Table S2). It is thus likely that extent of match to the consensus HSE, rather than presence of gap, step, or direct repeat HSEs *per se*, dictates Hsf1 binding avidity in vivo.

A mutual antagonism exists between Hsf1 and nucleosomes under NHS conditions

A striking observation is that the *HSP82* upstream regulatory region can be reconstituted into two sequence-positioned nucleosomes using only core histones and DNA. This chromatin structure, which recapitulates the dinucleosome present within the upstream region of *hsp82-ΔHSE1* (Gross *et al.*, 1993; Venturi *et al.*, 2000) and resembles the one reconstituted on a similar DNA sequence outfitted with p53 binding sites (Laptenko *et al.*, 2011), may actively antagonize Hsf1 binding. Indeed, under NHS conditions, Hsf1 binding is virtually undetectable at *hsp82-ΔHSE1*; instead, there is a three- to fourfold increase in histone H3 occupancy (Supplemental Figure S8). At *HSP82*$^{+}$ under NHS conditions, Hsf1 exists in a dynamic equilibrium with chromatin, as suggested by the cohabitation of Hsf1 with H2A, H2B, H3, and H4 (this study and Zhao *et al.* [2005]), creating a chromatin structure hypersensitive to DNase I cleavage (Gross *et al.*, 1990). Following acute heat shock, Hsf1's cooperative binding of HSEs (Erkine *et al.*, 1999), coupled with its recruitment of CRCs, HATs, and other coactivators (Kremer and Gross, 2009; Kim and Gross, 2013), leads to a 40-fold increase in nascent transcription and eviction of histones that extends across the gene (Supplemental Table S1; Supplemental Figure S8B) (Zhao *et al.*, 2005). Thus, the chromatin state of the *HSP82* promoter is subject to a dynamic remodeling process even under NHS conditions that is largely directed by Hsf1 itself.

Relationship to previous genomewide studies

It is instructive to compare findings reported here to previous genomewide studies of Hsf1 occupancy. Using ChIP microarray analysis, Thiele, Iyer and colleagues reported that *S. cerevisiae* Hsf1 binds 210 genomic sites, 165 of which were located upstream of distinct open reading frames and the majority of which were heat-inducibly bound by Hsf1 (Hahn *et al.*, 2004). Our ChIP-seq analysis, by contrast, identified only 74 genomic sites occupied by Hsf1, 69 of which were inducibly occupied and 46 of which were located upstream of genes whose heat-induced transcription was Hsf1 dependent. One explanation for the fewer genomic targets identified in our analysis is that we incorporated a high threshold for peak calls. This led to the exclusion of six genes likely occupied by Hsf1 since their heat-shock-induced transcription is Hsf1 dependent. However, this fact alone cannot entirely explain the disparity between the data sets, since only 31/43 core Hsf1 targets and 14/31 inducible targets identified here were also identified in the earlier ChIP-chip analysis. Holstege and colleagues examined Hsf1 occupancy in cells maintained under control, nonstressful conditions. Using ChIP-seq coupled with comparative dynamic transcription using Hsf1-AA strains, they identified 21 Hsf1 targets under NHS conditions (de Jonge *et al.*, 2017); we identify these same 21 genes using a combination of ChIP-seq, NAC-seq, and Anchor Away, plus four others (*HSP82*, *SSA2*, *SSA4*, and *UBI4*).

Several previous studies examined the interplay of nucleosomes and Hsf1 binding. In contrast to our observations, Brown and colleagues reported little loss of histone over the UAS/promoter regions of Hsf1-bound loci on heat shock of the pathogenic yeast *Candida albicans* (Leach *et al.*, 2016). Why this is the case is unclear but might be related to differential recruitment of CRCs. Similarly to findings reported here, *Drosophila* HSF occupancy was found to be strongly linked to preset chromatin that is nucleosome depleted, enriched in active histone marks, and whose landscape has prebound pioneer factors (Guertin and Lis, 2010). Most prominent of the pioneer factors identified was GAGA factor, whose roles include opening of promoter chromatin and facilitating the recruitment and pausing of Pol II (Fuda *et al.*, 2015). Following its heat-shock-induced binding, *Drosophila* HSF drives striking remodeling of chromatin (Petesch and Lis, 2008), as we have observed for yeast Hsf1. HSF also functions to release Pol II into the body of highly activated *HSP* genes (Duarte *et al.*, 2016). Likewise, in mammalian cells, heat shock activation of HSF1 target genes is regulated at the level of Pol II pause release (Mahat *et al.*, 2016), and HSF1 binding to both promoters and enhancers is accompanied by a marked increase in H4 acetylation (Vihervaara *et al.*, 2017).

These recent studies additionally suggest that only a fraction of all heat-shock-inducible genes in insects and mammals are under control of HSF1 (Duarte *et al.*, 2016; Mahat *et al.*, 2016). Likewise, in yeast, we observed that only 10% of heat-shock-inducible genes (i.e., those exhibiting greater than or equal to threefold increase in transcription) were Hsf1 dependent. Nonetheless, in each organism, the HSF1 regulon encompasses the *HSP* genes that encode chaperones and cochaperones, consistent with coevolution of the transcription factor, its cognate *cis*-response element, and a core set of target genes.

Conclusions

The results presented here point to three clear conclusions: 1) Yeast Hsf1, like metazoan HSFs, inducibly binds to its target promoters across the genome during acute heat shock, contrary to popular models that presume the existence of a fundamental difference in DNA-binding behavior. 2) There are a small number of essential chaperone genes to which Hsf1 binds strongly under NHS conditions; these genes have NFRs due to the presence of pioneer factors that expose strong HSEs. 3) Hsf1 expands its target regulon during heat shock by cooperating with CRCs to reveal HSEs occluded by nucleosomes, concomitant with driving its target genes—dispersed throughout the genome—into a coalesced, potentially phase-separated, state (Chowdhary *et al.*, 2017, 2018). Together, these mechanisms allow cells to dynamically control the breadth and magnitude of the heat shock response to tune the proteostasis network according to need.

MATERIALS AND METHODS

Yeast strains

Strains AJ1001, AJ1002, and AJ1003 are derivatives of SLY101, HSE102, and GRF200, respectively, in which *REB1* was C-terminally tagged with the Myc9 epitope as previously described (Kim and Gross, 2013). Similarly, ACY101 is a derivative of HHY212 (Haruki *et al.*, 2008) in which *STH1* was C-terminally tagged with the FRB domain. All other strains have been previously described (see Table 1).

Chromatin immunoprecipitation

ChIP experiments were performed as previously described (Kim and Gross, 2013) except as noted below. Mid–log cell cultures

Strain name	Genotype	Source or reference
BY4741	*MATa his3Δ1 leu2Δ0 met15Δ0 ura3Δ0*	Research Genetics
BY4742-Hsf1-AA	BY4741; *MATα tor1-1 fpr1Δ RPL13A-FKBP12::NAT MET15⁺ HSF1-FRB-yEGFP::KAN-MX*	F. Holstege, University Medical Center Utrecht, The Netherlands
SLY101	*MATα ade⁻ can1-100 cyh2ʳ his3-11,15 leu2-3,112 trp1-1 ura3*	Lee and Gross, 1993
HSE102	SLY101; *hsc82-ΔHSEs*	Erkine *et al.*, 1996
GRF200	SLY101; *hsc82-ΔREB1*	Erkine *et al.*, 1996
AJ1001	SLY101; *REB1-MYCx9::TRP1*	This study
AJ1002	HSE102; *REB1-MYCx9::TRP1*	This study
AJ1003	GRF200; *REB1-MYCx9::TRP1*	This study
KEY102	SLY101; *hsp82-ΔHSE1*	Gross *et al.*, 1993
KEY105	SLY101; *hsp82-ΔHSE1·*	Gross *et al.*, 1993
DPY1283	*MATα tpk1/2/3-as TOR1-1 fpr1Δ::NAT RPL13A-FKBP::TRP1 HSF1-FRB::HIS3 TEF2pr-mKate-4xHSE-EmGFP::URA3 RPB3-FLAG::KAN*	Solis *et al.*, 2016
HHY212	*MATa tor1-1 fpr1::loxP-LEU2-loxP RPL13A-2 × FKBP12::loxP-TRP1-loxP ade2-1 trp1-1 can1-100 leu2-3,112 his3-11,15 ura3-1*	Haruki *et al.*, 2008
ACY101	HHY212; *STH1-FRB::HIS3*	This study

TABLE 1: Yeast strains.

(350–500 ml), pregrown in YPDA medium (yeast extract-peptone-dextrose supplemented with 0.002% adenine) at 30°C, were used in both rapamycin (final concentration 1 μg/ml) and heat-shock time-course experiments. To effect a heat shock, an equal volume of prewarmed YPDA (50°–55°C) was added to each culture, instantaneously raising the temperature to 39°C. This was maintained thereafter in a shaking water bath. Aliquots (50 ml) were removed at each time point to which formaldehyde was added to a final concentration of 1% at the temperature of the treatment (30°C for NHS and 39°C for HS). Cells were harvested, washed, and resuspended in 250 μl lysis buffer and lysed with vigorous shaking in the presence of glass beads (~300 mg) at 4°C for 30 min. Cell lysates were then transferred to 1.5-ml TPX tubes and sonicated at 4°C using a Diagenode Biorupter Plus (50 cycles with 30 s pulses), generating chromatin fragments with a mean size of ~200–300 base pairs. TPX tubes were centrifuged to clarify supernatants that were then brought up to 2000 μl using ChIP lysis buffer. To perform immunoprecipitation, the equivalent of 500–800 μg chromatin protein (typically 200–400 μl) was incubated with one of the following antibodies: 1 μl of anti-Hsf1 (Erkine *et al.*, 1996), 2.5 μl of anti-Myc (Santa Cruz Biotechnology), and 1 μl of anti-H3 globular domain (Abcam; ab1791).

Immunoprecipitated DNA was resuspended in 60 μl TE (10 mM Tris-HCl, 0.5 mM EDTA, pH 8); 2 μl was used in quantitative PCR (qPCR) with Power SYBR Green PCR Master Mix (Applied Biosystems 4367660) on an Applied Biosystems 7900HT Real-Time PCR system. DNA was quantified using a standard curve specific for each amplicon, and background signal arising from beads alone was subtracted. Background was determined by signal arising from incubating an equivalent volume of chromatin extract with Protein A or Protein G–Sepharose beads (GE Healthcare Life Sciences; CL-4B or 4 Fast Flow, respectively). To normalize for variation in yield of chromatin extracts, in certain cases input was used. Briefly, 40 μl was removed from the 2000 μl chromatin lysate isolated as described above, and the volume was brought up to 400 μl. Formaldehyde-induced cross-links were reversed, and DNA was deproteinized as for ChIP samples. Purified Input DNA was dissolved in 300 μl TE, and 2 μl was removed for qPCR. The signal arising from this represents 2% of total input chromatin. In the case of H3 ChIP, signal at a test locus was normalized to that obtained at ARS504 as described (Zhang *et al.*, 2014). Primers used for detection and quantification of genomic loci in ChIP and Input DNAs are listed in Supplemental Table S3.

ChIP sequencing

ChIP-Seq experiments were performed as above except as noted below. BY4741 mid–log cell cultures (600 ml) were used for each heat-shock time-course sample (0-, 5-, and 120-min HS). Cells were harvested as 50-ml aliquots, with each pellet washed and resuspended in 250 μl lysis buffer and lysed with vigorous shaking in the presence of ~300 mg glass beads at 4°C for 30 min. Cell lysates were then transferred to 1.5-ml TPX tubes and sonicated at 4°C using a Diagenode Biorupter Plus (60 cycles with 30-s pulses). This procedure generates chromatin fragments with a mean size of 100–250 base pairs. TPX tubes were centrifuged to clarify supernatants that were pooled and brought up to 3000 μl using ChIP lysis buffer. To perform immunoprecipitation, 100 μl was incubated with 4 μl of anti-Hsf1 antiserum (Erkine *et al.*, 1996). As a control, 4 μl preimmune serum were used for each of the three time points. Five separate IPs were conducted for both the Hsf1 ChIP and the preimmune ChIP using 40 μl Protein A–Sepharose beads for each. Following purification of the IP and deproteinization, each ChIP DNA was suspended in 60 μl TE; the five samples were combined into one 300-μl pooled sample and quantified using the Qubit Fluorimeter assay. ChIP DNA (5 ng) was used to generate barcoded libraries using NEBNext Ultra DNA Library Prep Kit for Illumina (NEB E7370). Libraries were sequenced on Illumina Mi-Seq and NextSeq 500 instruments located in the LSUHSC Core Research Facility. Raw data are deposited on GEO; see *Data access* below.

Hsf1 ChIP-seq analysis

Reads were aligned to the SacCer3 build of the yeast genome using Bowtie2 (Langmead and Salzberg, 2012). We used MACS2 to call and quantify peaks, filtering for properly paired reads and controlling for nonspecific binding using condition-matched preimmune serum ChIP-seq data. We generated a signal file that outputs fragment pileups per million reads in bedgraph format (signal per

million mapped reads; SPMR). It was important that we allowed MACS2 (Zhang *et al.*, 2008) to model the expected value of duplicate reads (–keep dup auto) due the compact size of the genome and the high coverage of the data set. Only peaks that had SPMR summit values above the background threshold of 250 were designated Hsf1 targets. Motif enrichment analysis was performed using Multiple EM for Motif Elicitation (MEME)-ChIP (Ma *et al.*, 2014). The MACS command used for a generic sample/preimmune pair that had been fragmented to 180 base pairs:

macs2 callpeak -t SAMPLE.bam -c PREIMMUNE.bam -f BAMPE -g 1.2e7 -n SAMPLE -p 1e-3 –nomodel -B –SPMR –extsize 180 –keep-dup auto

We note that the algorithm calls a single motif under each peak (a contiguous sequence that has the closest match to consensus) and thus does not reveal existence of ancillary HSEs. These do, in fact, exist and can contribute to the cooperative binding of Hsf1 (e.g., *HSP82* [Erkine *et al.*, 1999]). We also note that when visualized using the Integrative Genomics Viewer (IGV) (Robinson *et al.*, 2011), small values often appear stretched and poorly reflect quantitative SPMR values (Figures 1B, 3, and 4 and Supplemental Figures S2 and S5, A–D). These are qualitative unless one zooms out so each peak is only in one pixel per bin.

Analysis of previously published NHS data sets

Histone modification and Htz1 ChIP-seq data were obtained from GSE61888 (Weiner *et al.*, 2015). Histone H3 data are from GSE74787 (Qiu *et al.*, 2016). Pioneer factor ChEC-seq data are from GSE67453 (Zentner *et al.*, 2015). As above, data were visualized using the IGV.

Nascent transcript sequencing

Nascent mRNA was enriched by purifying RNA that coprecipitates with RNA Pol II-component Rpb3. Hsf1 Anchor-Away cells expressing Rpb3-FLAG (strain DPY1283) were grown at 30°C to $OD_{600} = 0.8$ in YPD, treated ± 1 μM rapamycin for 45 min, and then harvested after a 5-min heat shock at 39°C (or mock-treated for an additional 5-min at 30°C [NHS sample]). Cells were collected and lysed in a coffee grinder as described (Zheng *et al.*, 2016) and resuspended in 1 ml IP buffer (20 mM HEPES, pH 7.4, 110 mM KOAc, 0.5% Triton X-100, 0.1% Tween-20, 10 mM $MnCl_2$, 1X Complete mini EDTA-free protease inhibitor, 50 U/ml SuperaseIn). DNA was digested with 150 U/ml RNase-free DNase for 20 min on ice and samples were centrifuged at 20,000 × *g*. Clarified lysate was added to 50 μl prewashed anti-FLAG M2 magnetic beads and incubated for 2 h at 4°C. Beads were washed four times with 1 ml IP buffer and eluted in 2 × 50 μl of 3xFLAG peptide (0.5 mg/ml) in IP buffer. RNA was purified using the Qiagen miRNeasy kit and libraries were prepared using the NEB Next Ultra RNA kit. Illumina sequencing libraries were sequenced at the Whitehead Genome Technology Core. Reads were aligned using Tophat, quantified with HTSeq-Count and normalized using DESeq2. A compilation of genomewide NAC-seq data is provided in Supplemental Table S1. Raw data are deposited at GEO; see *Data access*.

Reverse transcription–quantitative PCR (RT-qPCR)

Cells were cultivated in 600- to 650-ml mid–log cultures, and 50-ml aliquots were removed for each heat-shock time point and treated with 1/100th volume of 2 M sodium azide to terminate transcription. Total RNA was extracted using phenol-chloroform and purified using an RNeasy kit (Qiagen 74204). Purified RNA (0.5–2 μg) and random primers were used in each cDNA synthesis using the High-Capacity cDNA Reverse Transcription kit (Applied Biosystems 4368814). Synthesized cDNA was diluted 1:20, and 5 μl of diluted cDNA was added to each 20 μl real-time PCR. Relative cDNA levels were quantified by the delta delta (ΔΔ) Ct method. The Pol III transcript *SCR1* was used as a normalization control for quantification of *HSP* mRNA levels. PCR primers used to detect cDNAs are provided in Supplemental Table S3.

Nucleosome reconstitution and Hsf1 in vitro binding assay

For nucleosomal reconstitution of the *HSP82* upstream regulatory region, we amplified a 345-base-pair region spanning –353 to –9 (where +1 = ATG start codon) by PCR using a plasmid (KEM101) harboring the *HSP82 Eco*RI fragment (–1359 to +1543) as template. The forward primer was end labeled and gel purified. Reconstitution was achieved using the salt dilution method. Briefly, a 20-μl reaction containing 5 μg (2×10^6 cpm) of PCR fragment, 5 μg of unlabeled *Hae*III/*Msp*I-digested lambda DNA, and 10 μg HeLa histones were incubated in 15 mM Tris–HCl, pH 7.5, 5 M NaCl, 0.2 mM EDTA, 0.2 mM PMSF for 20 min at 37°C and then 5 min at room temperature (RT). At 10-min intervals thereafter, 10 μl of 15 mM Tris–HCl, pH 7.5, 0.2 mM EDTA, and 0.2 mM PMSF were added 18 times to a final volume of 200 μl. This mixture was then loaded onto a 7.5–35% glycerol gradient (3.75 ml total volume) and spun at 33,500 rpm in a Beckman L8 rotor for 15 h at 4°C. The gradient was fractionated into 25 equal volumes and 5 μl from each fraction were electrophoresed on a 5% polyacrylamide Tris–borate–EDTA gel. The fraction containing pure dinucleosomes (no free DNA, no chromatin aggregates) was used for footprinting (see Supplemental Figure S4).

To conduct DNase I footprinting, we challenged the template, either purified dinucleosome or free DNA, with recombinant Hsf1. GST-Hsf1, purified from *Escherichia coli* as previously described (Erkine *et al.*, 1999), was preincubated with ~125 ng dinucleosomal template (50,000 cpm) in 50 μl of 15 mM Tris–HCl, pH 7.5, 50 mM KCl, 4 mM $MgCl_2$ for 20 min at RT (0, 0.5, 1.5, 4.5, 13.5 ng GST-Hsf1 were used; see Figure 5B). In parallel, ~125 ng of naked DNA was similarly incubated with GST-Hsf1. A 1/100 dilution of DNase I (5 μl; Sigma D7291; 100 U/ μl stock) was then added to each mixture, and digestion was allowed to proceed for 2 min. It was terminated by addition of EDTA to 5 mM.

Data access

ChIP-seq and NAC-seq data sets can be accessed using GEO accession number GSE117653.

ACKNOWLEDGMENTS

We thank Amol Kainth for critical reading of the manuscript and assistance with data analysis; Paula Polk (LSUHSC Core Research Facility) for assistance with ChIP-seq; Tom Volkert and the Whitehead Institute Genome Technology Core for assistance with NAC-seq; Apeng Chen for strain construction; Jodi Taylor for assistance with data mining; and Frank Holstege for yeast strain BY4742-Hsf1-AA. This work was supported by an NIH Early Independence Award (DP5 OD017941) to D.P., a Feist-Weiller Postdoctoral Grant to J.A., and grants from the National Science Foundation (MCB-1518345) and National Institutes of Health (GM 128065) to D.S.G.

REFERENCES

Abravaya K, Myers MP, Murphy SP, Morimoto RI (1992). The human heat shock protein hsp70 interacts with HSF, the transcription factor that regulates heat shock gene expression. Genes Dev 6, 1153–1164.

Adams CC, Gross DS (1991). The yeast heat shock response is induced by the conversion of cells to spheroplasts and by potent transcriptional inhibitors. J Bacteriol 173, 7429–7435.

Bai L, Ondracka A, Cross FR (2011). Multiple sequence-specific factors generate the nucleosome-depleted region on CLN2 promoter. Mol Cell 42, 465–476.
Buchman AR, Lue NF, Kornberg RD (1988). Connections between transcriptional activators, silencers, and telomeres as revealed by functional analysis of a yeast DNA-binding protein. Mol Cell Biol 8, 5086–5099.
Cairns BR, Lorch Y, Li Y, Zhang M, Lacomis L, Erdjument-Bromage H, Tempst P, Du J, Laurent B, Kornberg RD (1996). RSC, an essential, abundant chromatin-remodeling complex. Cell. 87, 1249–1260.
Chasman DI, Lue NF, Buchman AR, LaPointe JW, Lorch Y, Kornberg RD (1990). A yeast protein that influences the chromatin structure of UAS_G and functions as a powerful auxiliary gene activator. Genes Dev 4, 503–514.
Chowdhary S, Kainth AS, Gross DS (2017). Heat shock protein genes undergo dynamic alteration in their three-dimensional structure and genome organization in response to thermal stress. Mol Cell Biol 37, e00292.
Chowdhary S, Kainth AS, Pincus DP, Gross DS (2018). Heat Shock Factor 1 drives intergenic association of its target gene loci upon heat shock. bioRxiv 400499.
Dai C, Whitesell L, Rogers AB, Lindquist S (2007). Heat shock factor 1 is a powerful multifaceted modifier of carcinogenesis. Cell 130, 1005–1018.
de Jonge WJ, O'Duibhir E, Lijnzaad P, van Leenen D, Groot Koerkamp MJ, Kemmeren P, Holstege FC (2017). Molecular mechanisms that distinguish TFIID housekeeping from regulatable SAGA promoters. EMBO J 36, 274–290.
Duarte FM, Fuda NJ, Mahat DB, Core LJ, Guertin MJ, Lis JT (2016). Transcription factors GAF and HSF act at distinct regulatory steps to modulate stress-induced gene activation. Genes Dev 30, 1731–1746.
Eastmond DL, Nelson HC (2006). Genome-wide analysis reveals new roles for the activation domains of the Saccharomyces cerevisiae heat shock transcription factor (Hsf1) during the transient heat shock response. J Biol Chem 281, 32909–32921.
Elfving N, Chereji RV, Bharatula V, Bjorklund S, Morozov AV, Broach JR (2014). A dynamic interplay of nucleosome and Msn2 binding regulates kinetics of gene activation and repression following stress. Nucleic Acids Res 42, 5468–5482.
Erkine AM, Adams CC, Diken T, Gross DS (1996). Heat shock factor gains access to the yeast *HSC82* promoter independently of other sequence-specific factors and antagonizes nucleosomal repression of basal and induced transcription. Mol Cell Biol 16, 7004–7017.
Erkine AM, Magrogan SF, Sekinger EA, Gross DS (1999). Cooperative binding of heat shock factor to the yeast *HSP82* promoter *in vivo* and *in vitro*. Mol Cell Biol 19, 1627–1639.
Fan X, Chou DM, Struhl K (2006). Activator-specific recruitment of Mediator in vivo. Nat Struct Mol Biol 13, 117–120.
Floer M, Wang X, Prabhu V, Berrozpe G, Narayan S, Spagna D, Alvarez D, Kendall J, Krasnitz A, Stepansky A, *et al*. (2010). A RSC/nucleosome complex determines chromatin architecture and facilitates activator binding. Cell 141, 407–418.
Fuda NJ, Guertin MJ, Sharma S, Danko CG, Martins AL, Siepel A, Lis JT (2015). GAGA factor maintains nucleosome-free regions and has a role in RNA polymerase II recruitment to promoters. PLoS Genet 11, e1005108.
Ganapathi M, Palumbo MJ, Ansari SA, He Q, Tsui K, Nislow C, Morse RH (2011). Extensive role of the general regulatory factors, Abf1 and Rap1, in determining genome-wide chromatin structure in budding yeast. Nucleic Acids Res 39, 2032–2044.
Gasch AP, Spellman PT, Kao CM, Carmel-Harel O, Eisen MB, Storz G, Botstein D, Brown PO (2000). Genomic expression programs in the response of yeast cells to environmental changes. Mol Biol Cell 11, 4241–4257.
Ghosh S, Pugh BF (2011). Sequential recruitment of SAGA and TFIID in a genomic response to DNA damage in Saccharomyces cerevisiae. Mol Cell Biol 31, 190–202.
Giardina C, Lis JT (1995). Dynamic protein-DNA architecture of a yeast heat shock promoter. Mol Cell Biol 15, 2737–2744.
Gomez-Pastor R, Burchfiel ET, Thiele DJ (2018). Regulation of heat shock transcription factors and their roles in physiology and disease. Nat Rev Mol Cell Biol 19, 4–19.
Gross DS, Adams CC, Lee S, Stentz B (1993). A critical role for heat shock transcription factor in establishing a nucleosome-free region over the TATA-initiation site of the yeast *HSP82* heat shock gene. EMBO J 12, 3931–3945.
Gross DS, English KE, Collins KW, Lee S (1990). Genomic footprinting of the yeast *HSP82* promoter reveals marked distortion of the DNA helix and constitutive occupancy of heat shock and TATA elements. J Mol Biol 216, 611–631.
Guertin MJ, Lis JT (2010). Chromatin landscape dictates HSF binding to target DNA elements. PLoS Genet 6, e1001114.
Hahn JS, Hu Z, Thiele DJ, Iyer VR (2004). Genome-wide analysis of the biology of stress responses through heat shock transcription factor. Mol Cell Biol 24, 5249–5256.
Hartley PD, Madhani HD (2009). Mechanisms that specify promoter nucleosome location and identity. Cell. 137, 445–458.
Haruki H, Nishikawa J, Laemmli UK (2008). The anchor-away technique, rapid, conditional establishment of yeast mutant phenotypes. Mol Cell 31, 925–932.
Hnisz D, Shrinivas K, Young RA, Chakraborty AK, Sharp PA (2017). A phase separation model for transcriptional control. Cell 169, 13–23.
Jakobsen BK, Pelham HRB (1988). Constitutive binding of yeast heat shock factor to DNA *in vivo*. Mol Cell Biol 8, 5040–5042.
Kim S, Gross DS (2013). Mediator recruitment to heat shock genes requires dual Hsf1 activation domains and Mediator Tail subunits Med15 and Med16. J Biol Chem 288, 12197–12213.
Krakowiak J, Zheng X, Patel N, Feder ZA, Anandhakumar J, Valerius K, Gross DS, Khalil AS, Pincus D (2018). Hsf1 and Hsp70 constitute a two-component feedback loop that regulates the yeast heat shock response. eLife 7, e31668.
Kremer SB, Gross DS (2009). SAGA and Rpd3 chromatin modification complexes dynamically regulate heat shock gene structure and expression. J Biol Chem 284, 32914–32931.
Krietenstein N, Wal M, Watanabe S, Park B, Peterson CL, Pugh BF, Korber P (2016). Genomic nucleosome organization reconstituted with pure proteins. Cell 167, 709–721.
Langmead B, Salzberg SL (2012). Fast gapped-read alignment with Bowtie 2. Nat Methods 9, 357–359.
Laptenko O, Beckerman R, Freulich E, Prives C (2011). p53 binding to nucleosomes within the p21 promoter in vivo leads to nucleosome loss and transcriptional activation. Proc Natl Acad Sci USA 108, 10385–10390.
Leach MD, Farrer RA, Tan K, Miao Z, Walker LA, Cuomo CA, Wheeler RT, Brown AJ, Wong KH, Cowen LE (2016). Hsf1 and Hsp90 orchestrate temperature-dependent global transcriptional remodelling and chromatin architecture in Candida albicans. Nat Commun 7, 11704.
Lee S, Gross DS (1993). Conditional silencing: The *HMRE* mating-type silencer exerts a rapidly reversible position effect on the yeast *HSP82* heat shock gene. Mol Cell Biol 13, 727–738.
Lee TI, Rinaldi NJ, Robert F, Odom DT, Bar-Joseph Z, Gerber GK, Hannett NM, Harbison CT, Thompson CM, Simon I, *et al*. (2002). Transcriptional regulatory networks in Saccharomyces cerevisiae. Science 298, 799–804.
Li B, Carey M, Workman JL (2007). The role of chromatin during transcription. Cell 128, 707–719.
Li J, Labbadia J, Morimoto RI (2017). Rethinking HSF1 in stress, development, and organismal health. Trends Cell Biol 27, 895–905.
Liu XD, Liu PC, Santoro N, Thiele DJ (1997). Conservation of a stress response: human heat shock transcription factors functionally substitute for yeast HSF. EMBO J 16, 6466–6477.
Lorch Y, Maier-Davis B, Kornberg RD (2014). Role of DNA sequence in chromatin remodeling and the formation of nucleosome-free regions. Genes Dev 28, 2492–2497.
Ma W, Noble WS, Bailey TL (2014). Motif-based analysis of large nucleotide data sets using MEME-ChIP. Nat Protoc 9, 1428–1450.
Mahat DB, Salamanca HH, Duarte FM, Danko CG, Lis JT (2016). Mammalian heat shock response and mechanisms underlying its genome-wide transcriptional regulation. Mol Cell 62, 63–78.
Mendillo ML, Santagata S, Koeva M, Bell GW, Hu R, Tamimi RM, Fraenkel E, Ince TA, Whitesell L, Lindquist S (2012). HSF1 drives a transcriptional program distinct from heat shock to support highly malignant human cancers. Cell 150, 549–562.
Neef DW, Jaeger AM, Gomez-Pastor R, Willmund F, Frydman J, Thiele DJ (2014). A direct regulatory interaction between chaperonin TRiC and stress-responsive transcription factor HSF1. Cell Rep 9, 955–966.
Neef DW, Jaeger AM, Thiele DJ (2011). Heat shock transcription factor 1 as a therapeutic target in neurodegenerative diseases. Nat Rev Drug Discov 10, 930–944.
Park JM, Werner J, Kim JM, Lis JT, Kim Y-J (2001). Mediator, not holoenzyme, is directly recruited to the heat shock promoter by HSF upon heat shock. Mol Cell 8, 9–19.
Petesch SJ, Lis JT (2008). Rapid, transcription-independent loss of nucleosomes over a large chromatin domain at Hsp70 loci. Cell 134, 74–84.

Qiu H, Chereji RV, Hu C, Cole HA, Rawal Y, Clark DJ, Hinnebusch AG (2016). Genome-wide cooperation by HAT Gcn5, remodeler SWI/SNF, and chaperone Ydj1 in promoter nucleosome eviction and transcriptional activation. Genome Res 26, 211–225.

Robinson JT, Thorvaldsdottir H, Winckler W, Guttman M, Lander ES, Getz G, Mesirov JP (2011). Integrative genomics viewer. Nat Biotechnol 29, 24–26.

Rougvie AE, Lis JT (1988). The RNA polymerase II molecule at the 5′ end of the uninduced *hsp70* gene of *D. melanogaster* is transcriptionally engaged. Cell 54, 795–804.

Sakurai H, Takemori Y (2007). Interaction between heat shock transcription factors (HSFs) and divergent binding sequences: binding specificities of yeast HSFs and human HSF1. J Biol Chem 282, 13334–13341.

Scherz-Shouval R, Santagata S, Mendillo ML, Sholl LM, Ben-Aharon I, Beck AH, Dias-Santagata D, Koeva M, Stemmer SM, Whitesell L, Lindquist S (2014). The reprogramming of tumor stroma by HSF1 is a potent enabler of malignancy. Cell 158, 564–578.

Shivaswamy S, Iyer VR (2008). Stress-dependent dynamics of global chromatin remodeling in yeast: A dual role for SWI/SNF in the heat shock stress response. Mol Cell Biol 28, 2221–2234.

Singh H, Erkine AM, Kremer SB, Duttweiler HM, Davis DA, Iqbal J, Gross RR, Gross DS (2006). A functional module of yeast Mediator that governs the dynamic range of heat-shock gene expression. Genetics 172, 2169–2184.

Solis EJ, Pandey JP, Zheng X, Jin DX, Gupta PB, Airoldi EM, Pincus D, Denic V (2016). Defining the essential function of yeast Hsf1 reveals a compact transcriptional program for maintaining eukaryotic proteostasis. Mol Cell 63, 60–71.

Sollner-Webb B, Melchior W, Jr, Felsenfeld G (1978). DNAase I, DNAase II and staphylococcal nuclease cut at different, yet symmetrically located, sites in the nucleosome core. Cell 14, 611–627.

Sorger PK, Lewis MJ, Pelham HRB (1987). Heat shock factor is regulated differently in yeast and HeLa cells. Nature 329, 81–84.

Sorger PK, Nelson HCM (1989). Trimerization of a yeast transcriptional activator via a coiled-coil motif. Cell 59, 807–813.

Venturi CB, Erkine AM, Gross DS (2000). Cell cycle-dependent binding of yeast heat shock factor to nucleosomes. Mol Cell Biol 20, 6435–6448.

Verghese J, Abrams J, Wang Y, Morano KA (2012). Biology of the heat shock response and protein chaperones: budding yeast (Saccharomyces cerevisiae) as a model system. Microbiol Mol Biol Rev 76, 115–158.

Vihervaara A, Mahat DB, Guertin MJ, Chu T, Danko CG, Lis JT, Sistonen L (2017). Transcriptional response to stress is pre-wired by promoter and enhancer architecture. Nat Commun 8, 255.

Vinayachandran V, Reja R, Rossi MJ, Park B, Rieber L, Mittal C, Mahony S, Pugh BF (2018). Widespread and precise reprogramming of yeast protein-genome interactions in response to heat shock. Genome Res 28, 357–366.

Weiner A, Hsieh TH, Appleboim A, Chen HV, Rahat A, Amit I, Rando OJ, Friedman N (2015). High-resolution chromatin dynamics during a yeast stress response. Mol Cell 58, 371–386.

Wu C (1995). Heat shock transcription factors: structure and regulation. Annu Rev Cell Dev Biol 11, 441–469.

Xiao H, Perisic O, Lis JT (1991). Cooperative binding of *Drosophila* heat shock factor to arrays of a conserved 5 bp unit. Cell 64, 585–593.

Zaret KS, Carroll JS (2011). Pioneer transcription factors: establishing competence for gene expression. Genes Dev 25, 2227–2241.

Zaret KS, Lerner J, Iwafuchi-Doi M (2016). Chromatin scanning by dynamic binding of pioneer factors. Mol Cell 62, 665–667.

Zentner GE, Kasinathan S, Xin B, Rohs R, Henikoff S (2015). ChEC-seq kinetics discriminates transcription factor binding sites by DNA sequence and shape in vivo. Nat Commun 6, 8733.

Zhang H, Gao L, Anandhakumar J, Gross DS (2014). Uncoupling transcription from covalent histone modification. PLoS Genetics 10, e1004202.

Zhang Y, Liu T, Meyer CA, Eeckhoute J, Johnson DS, Bernstein BE, Nusbaum C, Myers RM, Brown M, Li W, Liu XS (2008). Model-based analysis of ChIP-Seq (MACS). Genome Biol 9, R137.

Zhao J, Herrera-Diaz J, Gross DS (2005). Domain-wide displacement of histones by activated heat shock factor occurs independently of Swi/Snf and is not correlated with RNA polymerase II density. Mol Cell Biol 25, 8985–8999.

Zheng X, Krakowiak J, Patel N, Beyzavi A, Ezike J, Khalil A, Pincus D (2016). Dynamic control of Hsf1 during heat shock by a chaperone switch and phosphorylation. eLife 5, e18638.

Zou J, Guo Y, Guettouche T, Smith DF, Voellmy R (1998). Repression of heat shock transcription factor HSF1 activation by HSP90 (HSP90 complex) that forms a stress-sensitive complex with HSF1. Cell 94, 471–480.